International Journal of Nanomedicine

Dovepress
open access to scientific and medical research

Open Access Full Text Article

ORIGINAL RESEARCH

# Targeted hyperthermia after selective embolization with ferromagnetic nanoparticles in a $VX_2$ rabbit liver tumor model

This article was published in the following Dove Press journal:
International Journal of Nanomedicine
1 October 2013
Number of times this article has been viewed

Hongliang Sun[1]
Linfeng Xu[1]
Tianyuan Fan[2]
Hongzhi Zhan[3]
Xiaodong Wang[3]
Yanfei Zhou[2]
Ren-jie Yang[3]

[1]Department of Interventional Therapy, Sun Yat-Sen Memorial Hospital of Sun Yat-Sen University, Guangzhou, [2]Pharmacy School of Beijing University, Beijing, [3]Department of Interventional Therapy, Peking University School of Oncology, Beijing Cancer Hospital and Institute, Beijing, People's Republic of China



**Background:** The purpose of this study was to observe the effect and feasibility of hyperthermia and the influence of heat on surrounding organs in a $VX_2$ rabbit liver model exposed to an alternating magnetic field after embolization with ferromagnetic nanoparticles.

**Methods:** Forty rabbits containing implanted hepatic $VX_2$ carcinomas were divided into four groups, each containing ten rabbits. Fourteen days after tumor transplantation, we opened the abdomen to observe the size and shape of the tumor. A transfemoral retrograde approach was then used for hepatic arterial catheterization in groups B, C, and D to perform angiography and embolization. The next day, three rabbits in group B and all rabbits in group D were exposed to an alternating magnetic field, and the temperature was recorded simultaneously in the center of the tumor, at the edge of the tumor, and in the normal liver parenchyma. On day 28, all animals was euthanized to observe changes in the implanted liver tumor and the condition of the abdomen. A pathologic examination was also done.

**Results:** Before surgery, there was no significant difference in tumor volume between the four groups. Three different temperature points (center of the tumor, edge of the tumor, and in the normal liver parenchyma) of group B under an alternating magnetic field were 37.2°C ± 1.1°C, 36.8°C ± 1.2°C, and 36.9°C ± 2.1°C, none of which were significantly different from pretreatment values. Three points basal temperature in group D showed no significant difference ($F = 1.038$, $P = 0.413$). Seven to 26 minutes after hyperthermia, the temperature at the center of the tumor and at the edge of the tumor in group D was significantly different from the corresponding points in group B and from normal liver tissue in group D ($F_{\text{B–D center}} = 5.431$, $P_{\text{B–D center}} = 0.041$, $F_{\text{B–D edge}} = 9.744$, $P_{\text{B–D edge}} = 0.011$; $F_{\text{D}} = 8.379$, $P_{\text{D}} = 0.002$). The highest temperature recorded at the rim of the tumor was 46°C in group D. Fourteen days later, the tumor volume in the four groups was group A 31.4 ± 20.6 $cm^3$, group B 26.7 ± 18.2 $cm^3$, group C 28.7 ± 9.1 $cm^3$, and group D 25.8 ± 13.9 $cm^3$, with no significant difference found between the groups ($F = 0.218$, $P = 0.883$). The increase in tumor volume was greatest in group A and least in group D, while that in groups B and D was similar.

**Conclusion:** It is feasible to treat a $VX_2$ tumor in an alternating magnetic field after embolization with magnetic nanoparticles without a significant effect on the surrounding normal liver parenchyma.

**Keywords:** hyperthermia, ferromagnetic nanoparticles, Lipiodol®, hepatocellular carcinoma, animal model

Correspondence: Ren-jie Yang
Peking University School of Oncology, Beijing Cancer Hospital and Institue, Fucheng Road 52, Haidian District, Beijing 100142, People's Republic of China
Tel +86 10 8819 6324
Fax +86 20 8813 1600
Email renjieyang2007@163.com

## Introduction

For 80%–90% of patients with primary or secondary liver cancer, there is no opportunity to resect the lesions, so the prognosis was poor. Median survival is 3–6 months for patients with nonresectable hepatocellular carcinoma and 6–12 months for those with

nonresectable hepatic metastasis from colorectal cancer. Patients have to rely on various forms of treatment, including transarterial chemoembolization, transarterial infusion, physical or chemical ablation, chemotherapy, and other local treatments. Although these treatments have reasonable short-term efficacy, can relieve symptoms, and may occasionally downstage hepatic tumors to allow surgical resection, five-year survival, metastasis, and recurrence rates have not improved.

Compared with radiation and chemotherapy, hyperthermia is a physical therapy with few adverse effects and could be combined with other treatment strategies. It is known that sustained temperatures higher than 42°C cause necrosis of living cells. However, application of hyperthermia is limited by an inability to target tumor tissue and distribute heat accurately, and the inevitable damage done to the surrounding organs. Arterial embolization hyperthermia is an experimental modality which consists of selective arterial embolization with ferromagnetic particles and exposure to an external alternating magnetic field to generate hysteretic heat and treat tumor tissue in the liver. It is well established that hepatic cellular carcinoma obtains its blood supply mainly from the hepatic arterial system, whereas normal liver tissue receives most of its blood supply from the portal vein system. Therefore, arterial embolization hyperthermia may be a complementary treatment, with the advantages and disadvantages of transarterial chemoembolization and local hyperthermia.[1] In this study, we used a self-made magnetic nanomaterial and an alternating magnetic field to do the primary experiment.

# Materials and methods

## Animals

This experimental study was performed using New Zealand White rabbits aged 16–20 weeks and weighing 2.5 ± 0.4 kg. All work in this study was approved by the Peking University Health Science Center animal ethics committee (2006). On day 1, each rabbit was implanted with 1 $mm^3$ of tumor from an established $VX_2$ carcinoma line under laparotomy, with hepatic access gained via a 4 cm midline upper abdominal incision under barbiturate-induced general anesthesia.[2] The fresh tumor mass was taken from the hind limb of a rabbit used to pass the tumor cells to other subject, and implanted in the middle of the left lobe of the liver. Each rabbit was allowed to recover from general anesthesia after closure of the abdominal incision, and the tumor was then left to grow for 14 days.

## Ferromagnetic particles and equipment

The ferromagnetic nanoparticles used for arterial embolization hyperthermia in this study were prepared by the School of Pharmaceutical Sciences, Peking University Health Science Center, using a chemical precipitation method and consisted of magnetic iron oxide particles (20% $Fe_3O_4$, 50–150 nm in diameter), with 2.0 mL of these particles able to reach 80°C in an alternating magnetic field within 5 minutes in vitro[3–6] (Figures 1 and 2). The ferromagnetic nanoparticles were suspended in the same volume of Lipiodol® (Guerbet, Villepinte, France) using a 2.5 mL syringe and agitated for 2 minutes to form a suspension for subsequent hepatic arterial embolization.

A digital subtraction angiography device (Multistar TOP, Siemens Corporation, Washington, DC, USA) was used for transcatheter arterial embolization and a tumor magnetic induction hyperthermia system, developed by the Engineering Physics Department, Institute of Medical Physics, at Tsinghua University, was used for magnetic hyperthermia. Iopamidol (300mgI/ml, [Patheon Pharmaceutical Services Inc., Durham, NC, USA]) diluted with 1/3 dosage saline, Lipiodol, and a 1.8 or 2.3 French microcatheter (Tracker18, [Boston Scientific, Natick, MA, USA]/Radiomate, [S&G Biotech Inc, Gyeonggi-do, Korea]) were used for transcatheter arterial embolization.

## Treatment and control groups

Forty rabbits with 14-day-old implanted tumors were divided equally into four groups. The control group (group A) did not receive any treatment. Four weeks after tumor implantation, the rabbits were euthanized, their tumor diameters were measured, and the condition of the surrounding organs and number of metastases to the lungs were observed. The purpose of group A was to obtain dimensions for untreated tumors and compare them with those in the treatment groups.

Rabbits in group B (the group embolized using Lipiodol) underwent hepatic arterial embolization with Lipiodol alone. After embolization, three rabbits in this group were exposed to an alternating magnetic field (50 kA, 10 kHz), and the tem-

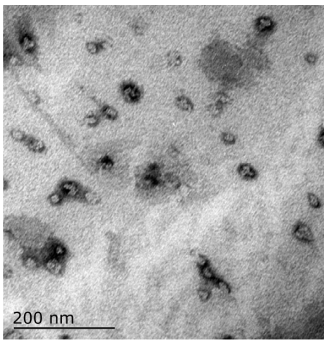


**Figure 1** Electron micrograph of nanoferromagnetic particles.

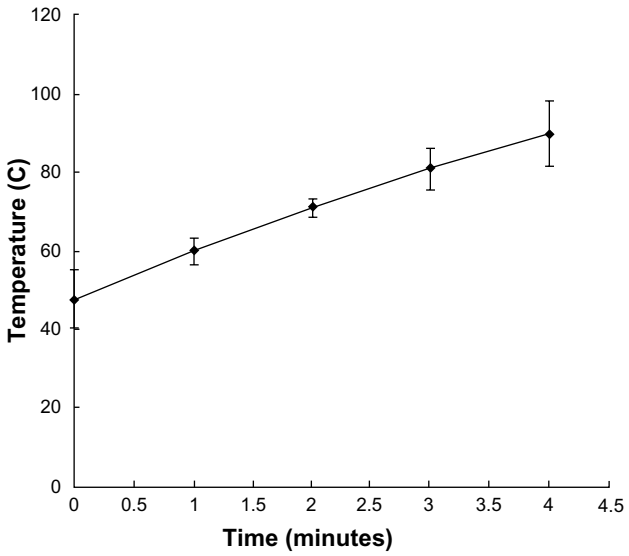


**Figure 2** Time-temperature curve under an alternating magnetic field in vitro ($Fe_3O_4$, 20%, 2 mL).

perature at the center of the tumor, at the edge of the tumor, and of the normal liver parenchyma were recorded automatically at one-minute intervals. After treatment, these three animals and others in group B were allowed to recover for 14 days.

Rabbits in group C (the group embolized using Lipiodol and a suspension of ferromagnetic particles) received embolization via catheterization of the hepatic artery. After treatment, each rabbit was allowed to recover for 14 days.

Rabbits in group D (artery embolization hyperthermia) received a hyperthermia treatment in an alternating magnetic field after embolized by magnetic particles and Lipiodol suspension. After treatment, each rabbit was allowed to recover for 14 days.

## Transarterial embolization

The experimental treatment was administered 14 days after tumor implantation. Each rabbit in groups B, C, and D underwent hepatic arterial catheterization under general anesthesia by intramuscular injection of ketamine 5 mg/kg mixed with 0.15 mL/kg of compound anesthetic agent 846 (containing haloperidol and dihydroetorphine), which was maintained by administration of compound anesthetic agent 846 at 0.1 mL/kg/hour. A 3 cm incision was made along the femoral artery sheath just under the groin. The right femoral artery was exposed, and the Seldinger method was used to insert a micro guidewire and catheter retrograde to the hepatic artery proper. Using digital subtraction angiography, the microcatheter was inserted as far as possible into the artery supplying blood to the tumor, and Lipiodol or a suspension containing the embolization agent was injected under fluoroscopy. Next, 0.2–0.3 mL of the embolization agent was infused slowly via a 1.0 mL syringe, followed immediately on each occasion by a heparin saline flush of 1.0 mL. Complete embolization was considered to have been achieved when the tumor was filled with the embolization agent and blood flow in the hepatic artery proper was slowed down. Group A was injected with 2.0 mL of saline only. The femoral artery was ligated proximal and distal to the point of puncture after removal of the microcatheter.

## Recording of temperature

For rabbits undergoing arterial embolization hyperthermia, fiber optic temperature probes were inserted surgically into the tumor center, the tumor rim, and the normal hepatic parenchyma. The temperature probes in the tumor and the normal hepatic parenchyma were fixed onto the abdominal wall. These probes recorded temperature every 60 seconds automatically onto a computer. The room temperature and basal temperature of the rabbits were also recorded before arterial embolization hyperthermia.

## Magnetic-mediated hyperthermia

Three rabbits in group B and all rabbits in group D were exposed to the alternating magnetic field to generate hyperthermia after embolization. After insertion of the temperature probes, the abdominal incision was sutured so that only the probe fibers penetrated the abdominal wall, thereby minimizing heat loss to the external environment. Under general anesthesia, the animal was placed into the open alternating magnetic field with dimensions of approximately 35 cm × 30 cm × 35 cm. After baseline temperatures were recorded, the magnetic field was initially set to 50 kA and 10 kHz; about 5 minutes later, the temperature reached its peak level and this was maintained for 25 minutes. Temperatures were recorded as the tissues cooled after the alternating magnetic field was shut down. The temperature in the center of the tumor was maintained between 42°C and 46°C for 20 minutes in the rabbits undergoing arterial embolization hyperthermia.

## Acquisition of histologic and blood specimens

A small tissue specimen was cut from the tumor rim and from the normal hepatic parenchyma just after arterial embolization hyperthermia in three subjects from each group for histologic investigation. Routine blood, liver, and kidney function tests was performed at baseline for each animal. Routine blood testing was repeated on day 7 after the experimental treatment and liver and kidney function tests were repeated on days 3 and 7.

Fourteen days after treatment, all rabbits were euthanized by barbiturate overdose. After dissection, the tumor size was measured and specimens of tumor and normal liver tissue were obtained. The condition of the organs of the abdomen and chest was observed at the same time. After hematoxylin and eosin staining, each specimen was observed under a microscope for necrosis and survival of tumor cells, as well as distribution of the ferromagnetic particles.

Three-dimensional vertical tumor diameters were measured for all animals on days 14 and 28 after tumor implantation. The formula applied to calculate tumor volume [1], and changes in volume [2], was as follows:

$$V = (a \times b \times c) \times \pi/6 \quad [1]$$

(where $V$ represents tumor volume, and $a$, $b$, and $c$ are the three-dimensional vertical diameters of the tumor)

$$T = \frac{V_{post\text{-}op} - V_{pre\text{-}op}}{V_{pre\text{-}op}} \quad [2]$$

(where $T$ represents increased multiples of tumor volume, $V_{post\text{-}op}$ is the post treatment tumor volume, and $V_{pre\text{-}op}$ is the tumor volume before treatment).

## Statistical analysis

All data were analyzed using Statistical Package for the Social Sciences version 13 software (SPSS Inc., Chicago, IL, USA). Means are expressed as $\overline{X} \pm SD$. One-way analysis of variance (ANOVA) was used to analyze the change in tumor volume before and after treatment and the change in temperature of the center of the tumor, edge of the tumor, and in the normal liver parenchyma. The Student's $t$-test was used to detect significant differences between two groups. Changes in routine bloods, liver function, and tumor biomarkers were analyzed using paired $t$-tests and one-way ANOVA. $P < 0.05$ (a = 0.05) was considered to indicate a statistically significant difference.

# Results

## Preparation of tumor model

All 40 rabbits underwent successful liver tumor implantation. There was no statistical difference in tumor volume between the four groups 14 days after implantation ($F$ = 1.403, $P$ = 0.259). The largest mean diameter in each treatment group was 1.5 ± 0.7 cm, 1.7 ± 0.7 cm, 1.9 ± 0.7 cm, and 2.1 ± 0.7 cm, and the mean tumor volume was 1.6 ± 1.5 $cm^3$, 2.5 ± 2.5 $cm^3$, 2.7 ± 1.6 $cm^3$, and 3.5 ± 2.6 $cm^3$, respectively for group A, group B, group C and group D.

## Angiography and embolization

All rabbits underwent angiography of the general and proper hepatic artery in eight of the rabbits the microcatheter was selectively inserted into the left hepatic artery. Angiography showed that the tumor was surrounded by an arterial blood supply, with obvious peripheral stain (Figure 3). After embolization, the embolization agent was deposited spherically in the area of the lesion, with a lesser amount deposited in the surrounding normal hepatic parenchyma (Figure 4). There was no statistically significant difference in the amount of embolization agent given to groups B, C, and D ($F$ = 1.356, $P$ = 0.241), and the dosage of the embolization agent used in these three groups was 0.66 ± 0.39 mL, 0.47 ± 0.12 mL, and 0.51 ± 0.1 mL, respectively.

One rabbit in group C and two rabbits in group D died at 16, 19, and 20 hours after embolization as a result of reflux of the embolization agent from the proper hepatic artery into the stomach, duodenal artery, or middle stomach artery. After dissection, it was found that there were perforations of different sizes on the gastric and duodenal anterior walls with irregular dark red ischemic zones (Figure 5). Two animals each in groups B, C, and D had an enlarged edematous gallbladder.

## Arterial embolization hyperthermia

Three rabbits in group B and eight rabbits in group D received hyperthermia in an alternating magnetic field after embolization. In group B, the mean basal temperature of the tumor center, tumor rim, and normal hepatic parenchyma was 37.1°C ± 1.3°C, 36.9°C ± 1.3°C, and 36.9°C ± 2.0°C, respectively, with no statistically significant difference in the temperatures recorded at the three sites ($F$ = 0.123, $P$ = 0.121); the mean temperatures recorded at the three sites in an alternating magnetic field were 37.2°C ± 1.1°C, 36.8°C ± 1.2°C,

**Figure 3** Angiography of the hepatic artery proper shows a clear rich blood supply to the tumor, especially at the rim.

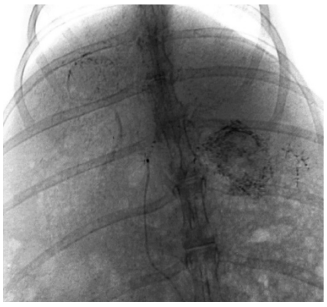

**Figure 4** Embolization with magnetic particles and Lipiodol®, with the agent deposited well in the lesion, and quite a few particles seen in the normal hepatic parenchyma.

and 36.9°C ± 2.1°C, respectively, and were not significantly different from the basal values ($F = 1.514$, $P = 0.512$).

In group D, the main basal temperature of the tumor center, tumor rim, and normal hepatic parenchyma was 35.4°C ± 1.7°C, 35.9°C ± 1.8°C, and 36.1°C ± 1.4°C, respectively, with no statistically significant difference in temperatures recorded at the three sites ($F = 1.514$, $P = 0.459$). After exposure to the alternating magnetic field, the temperature of the tumor center and tumor rim started to increase, reaching a peak after 5–10 minutes, and was maintained at that level. The maximum increase in temperature at the tumor rim was about 10°C–12°C, and the highest temperature recorded was 46°C. The temperature decreased to basal levels within 2–3 minutes of termination of exposure to the alternating magnetic field. The temperature of the normal hepatic parenchyma changed by less than 1°C. From 7 to 26 minutes, the temperature change at the tumor center and tumor rim was significantly different from that of the normal hepatic parenchyma in group D and at all three points in group B ($P < 0.05$, Table 1, Figures 6 and 7).

## Laboratory results

There were no statistically significant changes in the white blood cell (WBC) count in any of the groups before or after treatment ($t = -0.965$, $-0.610$, 1.812, and 1.125, all $P > 0.05$). Before treatment, the WBC count in the groups were $8.1 \pm 2.0 \times 10^9$/L, $8.1 \pm 3.2 \times 10^9$/L, $9.3 \pm 2.5 \times 10^9$/L, and $9.1 \pm 2.5 \times 10^9$/L, respectively for group A, group B, group C and group D, ($F = 0.534$, $P > 0.05$). Seven days after treatment, the respective WBC counts were $8.9 \pm 1.7 \times 10^9$/L, $8.8 \pm 1.7 \times 10^9$/L, $8.6 \pm 1.8 \times 10^9$/L, and $8.5 \pm 1.6 \times 10^9$/L ($F = 0.039$, $P > 0.05$).

Alanine aminotransferase and aspartate aminotransferase levels in groups B, C, and D on day 3 after treatment were much higher than pretreatment values, but these differences were not significantly different between the groups. Alanine aminotransferase and aspartate aminotransferase levels on day 3 after treatment in groups B, C, and D were significantly different from those before and 7 days after treatment (by pairwise comparison). Blood urea nitrogen (BUN) and blood creatinine (Cr) levels before and 7 days after treatment were not significantly different among the four groups ($F_{BUN} = 1.311$, $P_{BUN} = 0.287$; $F_{Cr} = 0.236$, $P_{Cr} = 0.871$). BUN and Cr levels on day 3 after treatment were a little higher than pretreatment levels ($P_{BUN(0-3d)} = 0.030$; $P_{Cr(0-3d)} = 0.027$), but returned to normal on day 7 after treatment ($P_{BUN(0-7d)} = 0.236$; $P_{Cr(0-7d)} = 0.894$, Table 2).

## Pathology

### Gross view

The tumor volume in group D increased more slowly than that in groups A, B, and C. In group D, the tissue in the lesion was harder than that of the normal hepatic parenchyma, and the surface of the tumor and surrounding tissue was dark as a result of exposure to the nanoparticles (Figure 8). Occasional abdominal lymph node enlargement was seen, along with mild peritoneal ascites. There were a few metastatic tubercles in the lungs, but no obvious abnormalities in the heart or kidneys.

Similar changes were seen in groups B and C. Tumor size in these two groups was larger than in group D, the surface of embolized liver lobe was granular like, and a yellow infarct area was visible. The greater omentum was adherent to the surface of the tumor, with a rich blood supply supporting the tumor. Blood-stained peritoneal ascites was common, with miliary or nodular metastases found in the lungs, along with hilar and retroperitoneal lymph node enlargement. However, black particles could only be seen on the tumor surface in group C.

The largest tumor size was seen in group A (Table 3). The tumors were often adherent to the abdominal wall or greater omentum, with gray flesh-like parenchyma and myxoid or cheese-like necrosis. There was much blood-stained peritoneal ascites, hilar retroperitoneal lymph node enlargement, and miliary or nodular metastases to the lungs.

**Figure 5** Perforations on stomach because of reflux of the mixed embolization agent.

**Table 1** Temperature at different tissue sites and times in groups B and D under an alternating magnetic field (°C)

| Groups site | Cases | Basic temperature | Time (minutes) | | | | | | |
|---|---|---|---|---|---|---|---|---|---|
| | | | 1 | 5 | 10 | 15 | 20 | 25 | 30 |
| Group B | 3 | | | | | | | | |
| Tumor center | | 37.1 ± 1.3 | 37.1 ± 1.7 | 37.1 ± 1.3 | 37.1 ± 1.4 | 37.2 ± 1.2[a] | 37.3 ± 1.1[a] | 37.5 ± 0.6[a] | 36.7 ± 1.8 |
| Tumor rim | | 36.9 ± 1.3 | 36.9 ± 1.6 | 37.0 ± 1.5 | 36.9 ± 1.5 | 36.8 ± 1.5[a] | 36.9 ± 1.4[a] | 36.7 ± 1.4[a] | 36.7 ± 1.2 |
| NHP | | 36.9 ± 2.0 | 37.0 ± 2.3 | 36.8 ± 2.5 | 36.8 ± 2.4 | 37.0 ± 2.6[a] | 37.0 ± 2.7[a] | 37.1 ± 2.7[a] | 37.1 ± 2.8 |
| Group D | 8 | | | | | | | | |
| Tumor center | | 35.4 ± 1.7 | 35.1 ± 2.2 | 35.3 ± 2.2 | 37.8 ± 2.5 | 40.1 ± 3.4 | 40.4 ± 2.9 | 40.9 ± 3.0 | 36.7 ± 3.0 |
| Tumor rim | | 35.9 ± 1.8 | 35.9 ± 1.9 | 36.3 ± 2.5 | 38.9 ± 3.6 | 42.5 ± 3.7 | 43.1 ± 3.5 | 43.5 ± 3.4 | 37.8 ± 4.3 |
| NHP | | 36.1 ± 1.4 | 36.2 ± 2.0 | 36.3 ± 1.9 | 36.5 ± 1.7 | 36.6 ± 1.7[a] | 36.7 ± 1.6[a] | 36.9 ± 1.6[a] | 36.2 ± 2.0 |
| $F_a$ | | | 0.750 | 0.535 | 1.768 | 5.528 | 7.418 | 7.280 | 0.372 |
| $P_a$ | | | 0.593 | 0.748 | 0.153 | 0.000 | 0.000 | 0.000 | 0.683 |

**Notes:** Group B, Lipiodol embolization group; group D, arterial embolization hyperthermia group. Tumor center temperature of group D compared with the three points of group B and NHP of group D at the same time point after the alternating magnetic field was turned on. [a]Statistically significant difference.
**Abbreviation:** NHP, normal hepatic parenchyma.

## Light microscopy

In group D, black particles filled in or attached to the wall of the small arterial vessel around the tumor, with a few particles seen to spread into the surrounding hepatic tissue. Many lymphocytes were seen spreading around the blood vessel, along with dead tumor cells (Figure 9). A number of magnetic particles were deposited in the normal hepatic parenchyma, but none were seen in the lungs. The distribution of particles in group C was similar to that in group D, with a small number of lymphocytes seen around the blood vessel, along with dead tumor cells. Lipiodol droplets were seen to be deposited in the blood vessel around the tumor in group B, with spread of lymphocytes and necrotic tumor cells as seen in group C. Necrotic areas and small tumor nests were seen spreading into the surrounding normal hepatic parenchyma, few fabric and lymph cells were seen in the tumors area in group A. The enlarged lymph nodes contained many tumor cells, and a number of metastatic nodules were seen to be present in both lungs.

## Tumor size

In all four groups, the most marked change in longest diameter and volume of tumors compared with pretreatment levels was seen 14 days after treatment. The greatest enlargement of tumor volume occurred in group A and the least in group D, while that in groups B and C was similar. However, the differences in tumor volume change between the four groups were not statistically significant ($P = 0.883$, Table 3).

# Discussion

## Principle of magnetic-mediated hyperthermia

Arterial embolization hyperthermia is one method of magnetic-mediated hyperthermia, and uses the arterial supply to the liver tumor to provide a pathway enabling selective embolization of the tumor with magnetic particles. Subsequent application of an external alternating magnetic field causes heating of the nanomagnetic particles by hysteresis or

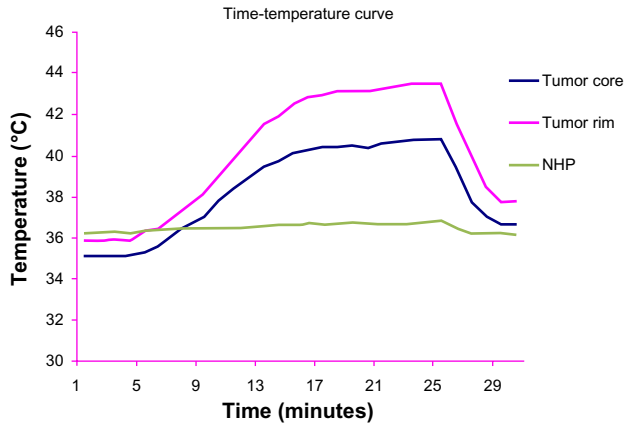


**Figure 6** Time-temperature curve for the three liver sites in group D in an alternating magnetic field.
**Abbreviation:** NHP, normal hepatic parenchyma.

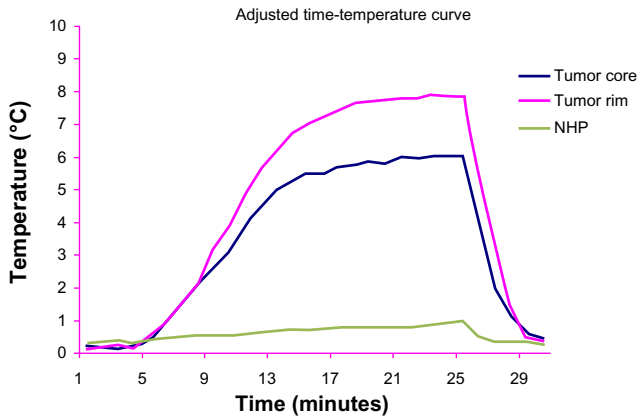


**Figure 7** Adjusted by basal temperature, time-temperature curve at the three liver sites in group D, in an alternating magnetic field.
**Abbreviation:** NHP, normal hepatic parenchyma.

**Table 2** Liver and kidney function in the four groups before and after treatment

| Groups | n | ALT (U/L) | AST (U/L) | BUN (mmol/L) | Cr (mmol/L) |
|---|---|---|---|---|---|
| Group A | 10 | | | | |
| Pretreatment | | 87.6 ± 40.9 | 48.3 ± 19.2 | 7.0 ± 1.4 | 64.3 ± 12.5 |
| Day 3 after treatment | | 77.9 ± 23.8 | 49.8 ± 13.2 | 7.6 ± 1.4 | 67.8 ± 10.3 |
| Day 7 after treatment | | 75.3 ± 22.7 | 50.7 ± 12.0 | 7.3 ± 1.1 | 59.7 ± 16.0 |
| *F* | | 0.458 | 0.064 | 0.488 | 0.952 |
| *P* | | 0.638 | 0.938 | 0.619 | 0.399 |
| Group B | 10 | | | | |
| Pretreatment | | 90.7 ± 48.6 | 40.8 ± 20.0 | 7.3 ± 1.1 | 64.2 ± 12.6 |
| Day 3 after treatment | | 641.8 ± 212.5 | 745.3 ± 174.4 | 7.2 ± 0.8 | 65.8 ± 12.3 |
| Day 7 after treatment | | 84.0 ± 17.3 | 59.8 ± 11.4 | 7.4 ± 0.7 | 60.0 ± 18.4 |
| *F* | | 63.953 | 156.263 | 0.114 | 0.415 |
| *P* | | 0.000 | 0.000 | 0.893 | 0.665 |
| Group C | 9 | | | | |
| Pretreatment | | 62.6 ± 22.3 | 39.9 ± 7.4 | 6.4 ± 1.2 | 65.0 ± 11.0 |
| Day 3 after treatment | | 643. 7 ± 164.7 | 762.4 ± 123.4 | 7.0 ± 1.2 | 64.7 ± 6.9 |
| Day 7 after treatment | | 75.6 ± 20.4 | 55.2 ± 10.8 | 6.9 ± 0.8 | 68.0 ± 12.8 |
| *F* | | 106.004 | 299.019 | 0.849 | 0.274 |
| *P* | | 0.000 | 0.000 | 0.44 | 0.763 |
| Group D | 8 | | | | |
| Pretreatment | | 98.2 ± 16.3 | 41.8 ± 14.1 | 6.5 ± 1.1 | 58.8 ± 7.3 |
| Day 3 after treatment | | 573.5 ± 209.0 | 694.2 ± 184.4 | 6.8 ± 1.0 | 62.5 ± 8.6 |
| Day 7 after treatment | | 84.8 ± 6.8 | 51.9 ± 12.5 | 6.7 ± 0.9 | 63.5 ± 6.0 |
| *F* | | 42.270 | 97.609 | 0.104 | 0.920 |
| *P* | | 0.000 | 0.000 | 0.902 | 0.414 |

**Notes:** ALT: compared among the four groups pretreatment ($F = 1.763$, $P = 0.173$); groups B, C, and D showed a significant difference from group A after treatment ($F = 23.981$, $P = 0.000$), with no difference between the three groups; ALT on day 3 was much higher than pretreatment and 7 days after treatment ($P < 0.05$) which returned to normal on day 7 ($P_{0-7d} = 0.41$). AST: compared among the four groups pretreatment ($F = 0.537$, $P = 0.660$); groups B, C, and D showed a significant difference from group A after treatment ($F = 58.518$, $P = 0.000$), with no significant difference between the three groups; on day 3, the AST level was much higher than pretreatment and 7 days after treatment ($P < 0.05$) which returned to normal on day 7, $P_{0-7d} = 0.113$. BUN: compared among the four groups pretreatment ($F = 1.073$, $P = 0.374$), no statistically significant difference between the four groups after treatment ($F = 1.311$, $P = 0.287$); on day 3, the BUN level was slightly higher than pretreatment ($P_{0-3d} = 0.030$), which returned to normal on day 7, $P_{0-7d} = 0.236$). Cr: compared among the four groups pretreatment ($F = 0.553$, $P = 0.650$); no statistically significant difference between the four groups after treatment ($F = 0.236$, $P = 0.871$); on day 3, the BUN level was slightly higher than pretreatment ($P_{0-3d} = 0.027$), which return to normal on day 7, $P_{0-7d} = 0.894$.
**Abbreviations:** ALT, alanine aminotransferase; AST, aspartate aminotransferase; BUN, blood urea nitrogen; Cr, blood creatinine.

Neel relaxation. The volume and position of the tumor does not affect the use of this modality, but can enhance the effect of heat after blocking blood flow, making this technique more advantageous than any of the other hyperthermia modalities. In our experiment, we used catheterization techniques identical to those used for human patients, giving the results more clinical relevance. The temperature reached during arterial embolization hyperthermia was 42°C–55°C, which was able to alter the function of many structural and enzymatic proteins within the tumor cells, in turn inhibiting cell growth and differentiation and inducing apoptosis. The magnetic particles did not deposit in normal hepatic parenchyma to any great extent, so arterial embolization hyperthermia would be unlikely to damage surrounding normal tissue. So, the character of conformal therapy was another advantage of arterial embolization hyperthermia, which other hyperthermia modalities do not have. Arterial embolization hyperthermia is a promising treatment, especially for hepatic cellular carcinoma.

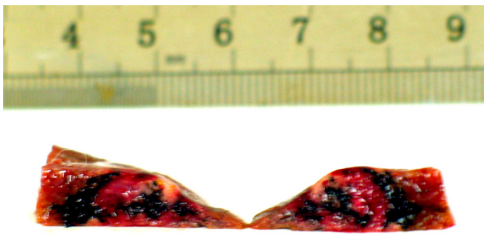


**Figure 8** Tumor section: inside and surrounding the tumor deposited a lot of black particles after magnetic embolization.

**Table 3** Longest tumor diameter and volume of tumor before and after treatment

| Group | n | Mean longest diameter (cm) | | Mean volume ($cm^3$) | |
|---|---|---|---|---|---|
| | | Pretreatment | Post treatment | Pretreatment | Post treatment |
| A | 10 | 1.6 ± 0.5 | 4.6 ± 1.1 | 1.6 ± 1.5 | 31.4 ± 20.6 |
| B | 10 | 1.8 ± 0.5 | 4.3 ± 1.1 | 2.5 ± 2.5 | 26.6 ± 18.2 |
| C | 9 | 1.9 ± 0.7 | 4.4 ± 0.5 | 2.7 ± 1.6 | 28.7 ± 9.1 |
| D | 8 | 2.1 ± 0.7 | 4.2 ± 0.6 | 3.5 ± 2.6 | 25.8 ± 13.9 |
| *F* | | 1.369 | 0.293 | 1.247 | 0.218 |
| *P* | | 0.260 | 0.830 | 0.457 | 0.883 |

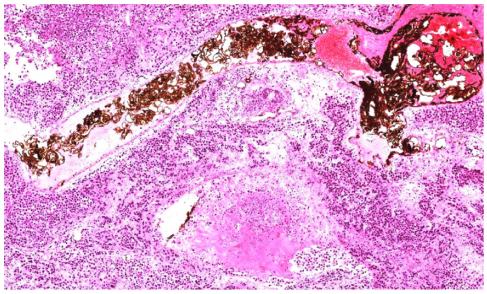

**Figure 9** Light microscope: small artery surrounding tumor filled with black particles, tumor cell around necrosis (HE, ×200).

## Effects of magnetic hyperthermia

### Change in tumor volume

Our experimental results show that tumor size in the control group 28 days after treatment was not significantly different from that in the other three groups. But concerning the increase in tumor volume, group A increased nearly 20 times, the largest increase observed in all groups, and group D had the smallest increase—only about eight times, while groups B and C were similar-nearly ten times. These findings indicate that the embolization reducing blood supply to the tumor could limit its growth, and magnetic hyperthermia after artery embolization by ferromagnetic particles had much more effect.

Both international[7–10] and local[11,12] researchers have reported that magnetic hyperthermia can suppress growth of implanted $VX_2$ tumors.[13,14] Although our experiment did not demonstrate a decrease in tumor volume, tumor growth was suppressed to some extent, and there are several possible explanations for this. First, $VX_2$ cells can invade widely and grow in numbers rapidly, so a few tumor cells can grow into a large tumor. Second, the thickness of the rabbit liver is not more than 2.0 cm, and if the size of tumor was large enough, it could reach the surface of the liver, stimulating the greater omentum to surround it, thereby obtaining an additional blood supply. Third, not all the tumor blood supply could be embolized, so the tumor was able to regain its blood supply and continue to grow after absorption of the embolization agent. Finally, a single administration of hyperthermia in an alternating magnetic field cannot destroy all tumor cells.[15]

### Temperature achieved by magnetic hyperthermia

In groups B and D, there were no statistically significant differences between or within the groups for temperatures measured at the tumor center, tumor rim, or normal hepatic parenchyma. Group B was embolized with Lipiodol only, which was unable to generate heat during hyperthermia, resulting in no temperature change at any of the three sites measured in the liver.

When mixed with Lipiodol, the concentration of the magnetic particles decreased, which slowed the rise in temperature. In group D, 5 minutes after the alternating magnetic field was switched on, temperatures in the center and rim of the tumor started to rise, and after 10–15 minutes, reached a peak of 45°C–46°C, which was maintained. The temperature at the tumor rim in one rabbit in group D increased by 12°C, while the temperature of the normal hepatic parenchyma in the right lobe of the liver increased by less than 1°C. The time-temperature curve for group D showed that the temperatures recorded in the tumor center and tumor rim were not exactly the same, with the temperature at the tumor rim being a little higher, which is different from what was found by other researchers,[16] who considered that the rim of the tumor was rich in capillaries supplying the tumor in contrast with the poor capillary blood supply in the center of the tumor, as shown on angiography of the hepatic artery. The distribution of capillaries leads to magnetic particles concentrating at the rim of the tumor, with few particles found in the central necrotic area (Figure 8).[17] Further, the thermoelectric temperature probes were so sensitive that they could detect small changes in temperature caused by magnetic particle distribution. For this reason, the temperature difference was about 2°C. In our study, the level of hyperthermia reached was able to suppress tumor growth. At the same time, there was a less than 1°C change in temperature in the normal hepatic parenchyma of the right lobe in group D, indicating that few magnetic particles are deposited in normal hepatic parenchyma during transarterial embolization and therefore do less harm to normal tissue.

## Pathology

The results showed that tumor size, volume of blood-stained ascites, abdominal lymph node enlargement, and numbers of lung metastases were less in group D than in the other three groups, indicating that, in addition to suppressing tumor growth, arterial embolization hyperthermia can reduce the number of metastases to some extent.

It was shown that arterial embolization hyperthermia inhibited tumor growth by not only killing tumor cells by heating but also by stimulating local infiltration of inflammatory cells. In group D, light microscopy showed that a small amount of magnetic particles spread into liver tissue, and inflammatory cells such as lymphocytes and monocytes were seen in the surrounding tissue, along with dead tumor cells and proliferation of fibrous tissue. The presence of

inflammatory cells is regarded as part of the body's reaction during suppression of tumor growth.

## Laboratory tests

There were no statistically significant differences in WBC count between or within the four groups before or 7 days after treatment. WBC counts returned to normal 7 days after treatment, and arterial embolization hyperthermia had no further influence on the blood count.

Compared with other embolization methods, arterial embolization hyperthermia has a limited effect on liver and kidney function, particularly with regard to the kidney. Three days after embolization, alanine aminotransferase and aspartate aminotransferase levels in groups B, C, and D appeared to be increased in comparison with pre-embolization levels. But there was no statistically significant difference among the three groups, which showed that mixed embolic agent and arterial embolization hyperthermia had no more damage on liver function. Liver function returned to normal on day 7 after treatment, indicating that arterial embolization hyperthermia did not deteriorate liver function. Except for slight increases on day 3, BUN and Cr levels showed no obvious change after treatment in any of the groups. Our findings in this regard are similar to those of other researchers.[18,19]

## Complications

As with any other embolization treatment administered via catheter, ectopic embolization was the most common complication in our study. The stomach, duodenum, and gallbladder were the organs most commonly affected. The gastroduodenal and mid gastric arteries were the two vessels in which reflux of the embolization agent occurred most often. There are three possible explanations for this reflux. First, the diameter of the hepatic artery proper in the rabbit is less than 0.5 mm, and the left hepatic artery is even narrower, which would cause blood flow to slow down after insertion of a microcatheter. Second, the microcatheter used in our study was a 1.8 French (0.6 mm diameter), which might obstruct hepatic blood flow after superselective catheterization and cause reflux of the embolization agent. Third, and important for reflux, was the speed at which the embolization was injected. Fourth, the mixed embolization agent was stickier. Under fluoroscopy it was shown as a strip but not an oil drop during injection. The agent attached to the inner wall of small arteries, causing an increase in friction and resistance, thereby promoting reflux.

Of note, reflux of Lipiodol alone did not lead to serious complications, but if the magnetic particles were mixed with the embolization agent, reflux caused gastric and duodenal perforation, followed by death of the rabbit. This observation suggests that the magnetic particles might cause more complete embolization than Lipiodol alone, and this possibility needs further in-depth study.

The other organ in which reflux was commonly seen was the gallbladder. The gallbladder artery usually originates from the right hepatic artery. It was very hard to perform superselective catheterization of the lobe artery or segmental artery because the left and right hepatic artery are very narrow in the rabbit. An embolization agent would inevitably flow into the gallbladder artery if the microcatheter could only reach the hepatic artery proper, and cause ischemic, edema, and even necrosis.[20]

In summary, the magnetic particles used in this study were able to heat tissue to therapeutic levels in an alternating magnetic field without a change of temperature in the surrounding organ tissue. Magnetic-mediated hyperthermia can suppress tumor growth and metastasis effectively, and is a promising treatment for liver cancer in the clinic.

# Acknowledgment

The staff of Tsinghua University are thanked for their assistance with this study.

# Disclosure

The authors report no conflicts of interest in this work.

# References

1. Moroz P, Jones SK, Gray BN. Magnetically mediated hyperthermia: current status and future directions. *Int J Hyperthermia*. 2002;18:267–281.
2. Zou Ch K, Liang HM, Li X, et al. [The preparation of $VX_2$ rabbit liver tumour model and the skill of artery catheterazition.] *Interventional Radiology*. 2006;15:101–104. Chinese.
3. Lu AH, Salabas EL, Schüth F. Magnetic nanoparticles: synthesis, protection, functionalization, and application. *Angew Chem Int Ed Engl*. 2007;46:1222–1244.
4. Wang X, Zhuang J, Peng Q, Li Y. A general strategy for nanocrystal synthesis. *Nature*. 2005;437:121–124.
5. Rauwel E, Galeckas A, Rauwel P, et al. Precursor-dependent blue-green photoluminescence emission of ZnO nanoparticles. *Phys Chem C*. 2011;115:2522–2527.
6. Wang ZY, Wang L, Zhang J, Li YT, Zhang DS. A study on the preparation and characterization of plasmid DNA and drug-containing magnetic nanoliposomes for the treatment of tumors. *Int J Nanomedicine*. 2011;6:871–875.
7. Kawashitaa M, Tanakab M, Kokubo T, et al. Preparation of ferrimagnetic magnetite microspheres for in situ hyperthermic treatment of cancer. *Biomaterials*. 2005;26:2231–2238.
8. Moroz P, Jones SK, Gray BN. Tumor response to arterial embolization hyperthermia and direct injection hyperthermia in a rabbit liver tumor model. *J Surg Oncol*. 2002;80:149–156.
9. Hu RL, Ma SL, Li H, et al. Effect of magnetic fluid hyperthermia on lung cancer nodules in a murine model. *Oncol Lett*. 2011;2:1161–1164.

10. Khandhar AP, Ferguson RM, Simon JA, Krishnan KM. Enhancing cancer therapeutics using size-optimized magnetic fluid hyperthermia. *J Appl Phys*. 2012;111:7B306–7B3063.
11. Yan Sh Y, Zhang D Sh, Deng J, et al. The nanometer magnetic fluid thermotherapy of $Fe_2O_3$ treats liver cancer. *Chinese Journal of Experimental Surgery*. 2004;12:1443–1446. Chinese.
12. Wang XM, Gu H Ch, Yang Zh Q, et al. Magnetism thermotherapy uses $Fe_3O_4$ heat effect in the reversal magnetic field. *Journal of Shanghai Jiaotong University*. 2005;2:275–278. Chinese.
13. Li XH, Rong PF, Jin HK, Wang W, Tang JT. Magnetic fluid hyperthermia induced by radiofrequency capacitive field for the treatment of transplanted subcutaneous tumors in rats. *Exp Ther Med*. 2012;3:279–285.
14. Bubnovskaya L, Belous A, Solopan A, et al. Nanohyperthermia of malignant tumors. II. In vivo tumor heating with manganese perovskite nanoparticles. *Exp Oncol*. 2012;34:336–339.
15. Ito A, Saito H, Mitobe K, et al. Inhibition of heat shock protein 90 sensitizes melanoma cells to thermosensitive ferromagnetic particle-mediated hyperthermia with low Curie temperature. *Cancer Sci*. 2009;100:558–564.
16. Moroz P, Jones SK, Gray BN. The effect of tumour size on ferromagnetic embolization hyperthermia in a rabbit liver tumour model. *Int J Hyperthermia*. 2002;18:129–140.
17. Alvarez-Berríos P, Castillo A, Mendéz J, et al. Hyperthermia potentiation of cisplatin by magnetic nanoparticle heaters is correlated with an increase in cell membrane fluidity. *Int J Nanomedicine*. 2013;8:1003–1013.
18. Yang Zh Q, Wang JH, Wang XM, et al. [The experiment of hyperthermia on $VX_2$ rabbit liver tumor after artery embolization with magnetic nanoparticles.] *Chinese Journal of Radiology*. 2006;8:870–874. Chinese.
19. Wang L, Dong J, Ouyang W, Wang X, Tang J. Anticancer effect and feasibility study of hyperthermia treatment of pancreatic cancer using magnetic nanoparticles. *Oncol Rep*. 2012;27:719–726.
20. Lévy M, Wilhelm C, Siaugue JM, Horner O, Bacri JC, Gazeau F. Magnetically induced hyperthermia: size-dependent heating power of γ-Fe(2)O(3) nanoparticles. *J Phys Condens Matter*. 2008;20:204133.